

# Formation of oxide phases in the system $\text{Fe}_2\text{O}_3\text{--NiO}$

S. MUSIĆ, S. POPOVIĆ\*, S. DALIPI

Rudjer Bošković Institute, P.O. Box 1016, 41001 Zagreb\*, \*Physics Department, Faculty of Science, P.O. Box 162, 41001 Zagreb, Republic of Croatia

Mixed metal oxides in the system  $\text{Fe}_2\text{O}_3\text{--NiO}$  were prepared by coprecipitation of  $\text{Fe}(\text{OH})_3/\text{Ni}(\text{OH})_2$  and the thermal treatment of hydroxide coprecipitates up to 800 or 1100 °C. X-ray diffraction showed the presence of  $\alpha\text{-Fe}_2\text{O}_3$ , NiO and  $\text{NiFe}_2\text{O}_4$  in samples prepared at 800 °C. The oxide phases  $\alpha\text{-Fe}_2\text{O}_3$ , NiO,  $\text{NiFe}_2\text{O}_4$  and a phase with structure similar to  $\text{NiFe}_2\text{O}_4$  were found in samples prepared at 1100 °C. Fourier transform–infrared spectra of oxide phases formed in the system  $\text{Fe}_2\text{O}_3\text{--NiO}$  are discussed. Two very strong infrared bands at 553 and 475  $\text{cm}^{-1}$ , a weak intensity infrared band at 383  $\text{cm}^{-1}$  and two shoulders at 626 and 441  $\text{cm}^{-1}$  were observed for  $\alpha\text{-Fe}_2\text{O}_3$  prepared at 1100 °C.  $\text{NiFe}_2\text{O}_4$ , prepared at the same temperature, showed two broad and very strong infrared bands at 602 and 411  $\text{cm}^{-1}$ , while NiO showed a broad infrared band at 466  $\text{cm}^{-1}$ . Fourier transform–infrared spectroscopic results were in agreement with X-ray diffraction.

## 1. Introduction

Mixed metal oxides, prepared in the system  $\text{Fe}_2\text{O}_3\text{--NiO}$ , have been investigated from different points of view.

Sitakara Rao *et al.* [1] investigated transformations of iron(III)–nickel(II) mixed oxide gels. The experimental results indicated that addition of  $\text{Ni}^{2+}$  ions to  $\text{Fe}^{3+}$  solution created unfavourable conditions for the formation of  $\alpha\text{-FeOOH}$ . The mixed oxide gels containing more than 2 mol % NiO did not show the presence of  $\alpha\text{-FeOOH}$ . Differential thermal analysis (DTA) results suggested the formation of a solid solution between  $\text{Fe}_2\text{O}_3$  and NiO up to 2 mol % NiO, and of nickel ferrite,  $\text{NiFe}_2\text{O}_4$ , at a higher concentration of NiO. At the stoichiometric ratio for  $\text{NiFe}_2\text{O}_4$  formation, a nickel ferrite precursor was formed at  $\sim 185^\circ\text{C}$ , which further transformed to amorphous ferrite at  $\sim 275^\circ\text{C}$  and above 400 °C to crystalline nickel ferrite.

Tamura *et al.* [2] investigated the formation of  $\text{Fe}_3\text{O}_4$  and  $\text{NiFe}_2\text{O}_4$  films in aqueous solutions at 100–200 °C. In solutions containing  $\text{FeCl}_2$  and  $\text{NaNO}_2$ , two phases,  $\text{Fe}_3\text{O}_4$  and  $\alpha\text{-Fe}_2\text{O}_3$ , were formed. Addition of  $\text{Ni}^{2+}$  ions to  $\text{FeCl}_2 + \text{NaNO}_2$  solution created conditions for the formation of nickel ferrite. The  $\text{Ni}^{2+}$  content in nickel ferrite was dependent on starting concentration of  $\text{NiCl}_2$  and the temperature of ferrite formation.

Spherical and hollow  $\text{NiFe}_2\text{O}_4$  particles were prepared using the aerosol technique [3]. A dilute aqueous solution of  $\text{Ni}(\text{NO}_3)_2 + \text{Fe}(\text{NO}_3)_3$ , with stoichiometric ratio for  $\text{NiFe}_2\text{O}_4$  formation, was used for the production of aerosols. The aerosol droplets were thermally treated at 450–810 °C. Particle-size distribution, degree of crystallinity of  $\text{NiFe}_2\text{O}_4$  particles and

their magnetic behaviour, were dependent on the temperature of pyrolysis.

Ibrahim and El-Shobaky [4] investigated the effects of  $\text{Li}_2\text{O}$  doping on the interaction between  $\alpha\text{-Fe}_2\text{O}_3$  and basic nickel carbonate. Doping with  $\text{Li}_2\text{O}$  enhanced the formation of  $\text{NiFe}_2\text{O}_4$  to an extent proportional to the amount of  $\text{Li}_2\text{O}$  added. These authors [4] concluded that  $\text{Li}_2\text{O}$  doping stimulated the formation of  $\text{NiFe}_2\text{O}_4$ , due to an increase in the mobility of the reacting cations.

MacKenzie and Cardile [5] investigated the formation of  $\text{NiFe}_2\text{O}_4$  from haematite, magnetite or spinel ironsand which was found on the West coast of the North Island of New Zealand. All three starting materials reacted with NiO producing  $\text{NiFe}_2\text{O}_4$ . The spinels formed from haematite, magnetite or ironsand and NiO in an inert atmosphere had larger lattice parameters than the corresponding air-reacted samples indicating the presence of  $\text{Fe}^{2+}$  in ferrite structure. Mössbauer spectroscopy suggested that the  $\text{Fe}^{2+}$  in the ferrite structure is located preferentially in the octahedral sites. It was also concluded that the  $\text{NiFe}_2\text{O}_4$  formed in air was not fully inverse as is usually assumed, and that it contained varying amounts of tetrahedral  $\text{Ni}^{2+}$ .

Mixed metal oxides,  $\text{Fe}_2\text{O}_3\text{--NiO}$ , containing up to 5 mol % NiO, were prepared by sintering the corresponding oxides at 1050–1300 °C [6]. It was concluded that the addition of NiO changed the majority of charge carriers in the  $\text{Fe}_2\text{O}_3$  from n to p-type. In samples containing more than 0.5 mol % NiO, the electrical conductivity was strongly influenced by the formation of nickel ferrite.

Mössbauer spectroscopy was used to study magnetic properties of small  $\text{NiFe}_2\text{O}_4$  particles [7, 8].

$^{57}\text{Fe}$  Mössbauer spectra of  $\text{NiFe}_2\text{O}_4$  were recorded, when a longitudinal magnetic field was applied. The spectra indicated a non-collinear magnetic structure of small  $\text{NiFe}_2\text{O}_4$  particles. The experimental results also indicated the importance of the particle morphology which must be taken into account in any detailed analysis of the surface magnetism. The authors of these papers [7, 8] proposed the model in which the  $\text{NiFe}_2\text{O}_4$  particles consisted of a core with the usual spin arrangement and a surface layer with atomic moments inclined to the direction of the net magnetization. Similar results were obtained for  $\gamma\text{-Fe}_2\text{O}_3$  and  $^{57}\text{Fe}\text{-CrO}_2$  particles [9].

Allen *et al.* [10] investigated structural properties of spinels containing nickel, chromium and iron, which were prepared by the solid state reactions of the corresponding metal oxides in an atmosphere of  $\text{CO}_2$  or  $\text{CO}_2/2\% \text{CO}$  at  $950^\circ\text{C}$ .

Oxidation products formed on stainless steel 18Cr-10Ni-2Mn at  $900\text{--}1100^\circ\text{C}$  were studied using X-ray diffraction, conversion electron Mössbauer spectroscopy (CEMS) and Fourier transform-infrared spectroscopy (FT-IR) [11]. The oxidation products on the steel surface,  $\text{Cr}_2\text{O}_3$ ,  $\text{MnCr}_2\text{O}_4$  and  $\alpha\text{-Fe}_2\text{O}_3$ , were detected. However,  $\text{NiFe}_2\text{O}_4$ , NiO or  $\text{NiCr}_2\text{O}_4$  were not detected in oxide layers.

The aim of the present work was to obtain further information about chemical and structural properties of oxide phases formed in the system  $\text{Fe}_2\text{O}_3\text{-NiO}$ . The samples were prepared by gradually changing the molar contents of  $\text{Fe}_2\text{O}_3$  and NiO components over the whole concentration range. X-ray diffraction and FT-IR spectroscopy were used as experimental techniques. In our previous works [12, 13] it was proved that vibrational spectroscopy was a very useful technique for detection of chemical and structural changes in mixed metal oxides.

## 2. Experimental procedure

Analar reagent grade chemicals and doubly distilled water were used for the preparation of samples. Mixed metal hydroxides were obtained by addition of

TABLE I Chemical composition of the samples prepared in the system  $\text{Fe}_2\text{O}_3\text{-NiO}$

Sample	Molar fraction	
	$\text{Fe}_2\text{O}_3$	NiO
S-1, S-1*	1	
S-2, S-2*	0.99	0.01
S-3, S-3*	0.975	0.025
S-4, S-4*	0.95	0.05
S-5, S-5*	0.90	0.10
S-6, S-6*	0.80	0.20
S-7, S-7*	0.50	0.50
S-8, S-8*	0.20	0.80
S-9, S-9*	0.10	0.90
S-10, S-10*	0.05	0.95
S-11, S-11*	0.025	0.975
S-12, S-12*	0.01	0.99
S-13, S-13*		1

NaOH solution to  $\text{Fe}(\text{NO}_3)_3 + \text{Ni}(\text{NO}_3)_2$  solution.  $\text{Fe}(\text{OH})_3/\text{Ni}(\text{OH})_2$  coprecipitates were carefully washed using a Sorvall RC2-B ultra-speed centrifuge (20 000 r.p.m.). After drying, the hydroxide coprecipitates were heated as follows: 1 h at  $200^\circ\text{C}$ , 1 h at  $300^\circ\text{C}$ , 1 h at  $400^\circ\text{C}$  and 5 h at  $800^\circ\text{C}$  ("step-by-step" heating). These samples were additionally heated for 1 h at  $1100^\circ\text{C}$  in a high-temperature furnace LKO II with Kanthal heaters. The samples heated at  $1100^\circ\text{C}$  are labelled with an asterisk. The chemical composition of 26 samples, S-1 to S-13 and S-1\* to S-13\*, is given in Table I.

X-ray diffraction powder patterns were taken at room temperature using a counter diffractometer with monochromatized  $\text{CuK}_\alpha$  radiation (Philips diffractometer, proportional counter and graphite monochromator).

All FT-IR spectra were recorded using a Fourier transform-IR spectrometer, model 1720-x (Perkin-Elmer). The specimens were pressed in KBr discs. In this paper, the FT-IR spectra are presented as relative transmittance versus the wave number ( $\text{cm}^{-1}$ ).

## 3. Results and discussion

The crystalline phases found in the system  $\text{Fe}_2\text{O}_3\text{-NiO}$  were identified according to the data given in the literature [14]. Crystallographic data for  $\alpha\text{-Fe}_2\text{O}_3$ , NiO,  $\text{NiFe}_2\text{O}_4$  and  $(\text{Ni, Fe})\text{Fe}_2\text{O}_4$  are summarized in Table II.

The unit-cell parameter of  $\text{NiFe}_2\text{O}_4$  is very close to twice as large as that of NiO. Both compounds possess the fcc crystal structure and for this reason, NiO does not exhibit independent diffraction lines of  $\text{NiFe}_2\text{O}_4$ .  $\text{NiFe}_2\text{O}_4$  by itself exhibits some independent diffraction lines. No separation between overlapped diffraction lines of these two compounds was detected for samples where both compounds were present, even at high Bragg angles. For such samples the changes in fractions of NiO and  $\text{NiFe}_2\text{O}_4$  can be followed by comparison of the intensities of overlapped diffraction lines belonging to both compounds with the intensities of diffraction lines belonging only to  $\text{NiFe}_2\text{O}_4$ .

TABLE II Crystallographic data for  $\alpha\text{-Fe}_2\text{O}_3$ , NiO,  $\text{NiFe}_2\text{O}_4$  and  $(\text{Ni, Fe})\text{Fe}_2\text{O}_4$  [14] at room temperature

JCPDS-PDF card no.	Compound	Space group	Unit-cell parameters at $25^\circ\text{C}$ (nm)
13-534	$\alpha\text{-Fe}_2\text{O}_3$	$R\bar{3}c$ (no. 167)	Hexagonal axes: $a = 0.5034$ $c = 1.3752$
10-325	$\text{NiFe}_2\text{O}_4$ (synthetic sample)	$Fd\bar{3}m$ (227)	$a = 0.8339$
23-1119	$(\text{Ni, Fe})\text{Fe}_2\text{O}_4$ (mineral trevorite)	$Fd\bar{3}m$ (227)	$a = 0.8367$
4-835	NiO	$Fm\bar{3}m$ (225)	$a = 0.41769$

TABLE III X-ray diffraction phase analysis of samples in the system  $\text{Fe}_2\text{O}_3$ -NiO heated at a maximum temperature of 800 °C

Sample	Molar fraction of NiO	Phase composition (approximate molar fraction)
S-1	0	$\alpha\text{-Fe}_2\text{O}_3$
S-2	0.01	$\alpha\text{-Fe}_2\text{O}_3$
S-3	0.025	$\alpha\text{-Fe}_2\text{O}_3 + \text{NiFe}_2\text{O}_4$ (< 0.01)
S-4	0.05	$\alpha\text{-Fe}_2\text{O}_3 + \text{NiFe}_2\text{O}_4$ (0.01)
S-5	0.10	$\alpha\text{-Fe}_2\text{O}_3 + \text{NiFe}_2\text{O}_4$ (0.02)
S-6	0.20	$\alpha\text{-Fe}_2\text{O}_3 + \text{NiFe}_2\text{O}_4$ (0.25)
S-7	0.50	$\text{NiFe}_2\text{O}_4 + \alpha\text{-Fe}_2\text{O}_3$ (0.02)
S-8	0.80	$\text{NiFe}_2\text{O}_4 + \text{NiO}$ (0.20)
S-9	0.90	$\text{NiFe}_2\text{O}_4 + \text{NiO}$ (0.35)
S-10	0.95	$\text{NiO} + \text{NiFe}_2\text{O}_4^a$ (0.15)
S-11	0.975	NiO
S-12	0.99	NiO
S-13	1	NiO

<sup>a</sup> Broadened diffraction lines.

TABLE IV X-ray diffraction phase analysis of samples in the system  $\text{Fe}_2\text{O}_3$ -NiO heated at maximum temperature of 1100 °C

Sample	Molar fraction of NiO	Phase composition (approximate molar fraction)
S-1*	0	$\alpha\text{-Fe}_2\text{O}_3$
S-2*	0.01	$\alpha\text{-Fe}_2\text{O}_3 + \text{"NiFe}_2\text{O}_4\text{"}^a$ (0.01)
S-3*	0.025	$\alpha\text{-Fe}_2\text{O}_3 + \text{"NiFe}_2\text{O}_4\text{"}$ (0.03)
S-4*	0.05	$\alpha\text{-Fe}_2\text{O}_3 + \text{"NiFe}_2\text{O}_4\text{"}$ (0.10)
S-5*	0.10	$\alpha\text{-Fe}_2\text{O}_3 + \text{"NiFe}_2\text{O}_4\text{"}$ (0.20)
S-6*	0.20	$\alpha\text{-Fe}_2\text{O}_3 + \text{"NiFe}_2\text{O}_4\text{"}$ (0.25)
S-7*	0.50	$\text{NiFe}_2\text{O}_4$
S-8*	0.80	$\text{NiFe}_2\text{O}_4 + \text{NiO}$ (0.15)
S-9*	0.90	$\text{NiFe}_2\text{O}_4 + \text{NiO}$ (0.35)
S-10*	0.95	$\text{NiO} + \text{NiFe}_2\text{O}_4$ (0.35)
S-11*	0.975	$\text{NiO} + \text{NiFe}_2\text{O}_4$ (0.15)
S-12*	0.99	$\text{NiO} + \text{NiFe}_2\text{O}_4$ (0.05)
S-13*	1	NiO

<sup>a</sup> "NiFe<sub>2</sub>O<sub>4</sub>" represents a phase having a structure similar to that of NiFe<sub>2</sub>O<sub>4</sub>.

The unit-cell parameters of  $\alpha\text{-Fe}_2\text{O}_3$  (samples S-1 and S-1\*) and NiO (samples S-13 and S-13\*) measured in this work were practically equal to the literature data given in Table II. For this reason, the literature data were used for calibration of the angular scale of the diffractometer.

The results of X-ray diffraction phase analysis are summarized in Tables III and IV. It can be seen that the structural characteristics of the samples depended on the maximum heating temperature. For samples prepared at 800 °C the fraction of  $\alpha\text{-Fe}_2\text{O}_3$  decreased from sample S-1 to sample S-7. In sample S-6,  $\alpha\text{-Fe}_2\text{O}_3$  was dominant, while in sample S-7,  $\alpha\text{-Fe}_2\text{O}_3$  was present only with a few per cent. In samples S-8 to S-12,  $\alpha\text{-Fe}_2\text{O}_3$  was not detected.  $\alpha\text{-Fe}_2\text{O}_3$  exhibited sharp diffraction lines, which did not change their angular positions, over the whole interval, from sample S-1 to sample S-7.

The phase NiFe<sub>2</sub>O<sub>4</sub> appeared in sample S-3 and its fraction increased up to sample S-7, where it was dominant. Then NiFe<sub>2</sub>O<sub>4</sub> fraction decreased up to

sample S-10. In samples S-8 and S-9, NiFe<sub>2</sub>O<sub>4</sub> was also dominant, while in sample S-10 it exhibited rather broad diffraction lines. NiFe<sub>2</sub>O<sub>4</sub> was not detected in samples S-11 and S-12. Diffraction lines of NiFe<sub>2</sub>O<sub>4</sub> practically did not change their positions in the interval from sample S-6 to sample S-10. The same might also be concluded for the interval from sample S-3 to sample S-5, although diffraction lines of NiFe<sub>2</sub>O<sub>4</sub> in these samples were rather faint.

NiO appeared in sample S-8, its fraction increased to sample S-13, and it was already a dominant component in sample S-10. NiO exhibited sharp diffraction lines, which did not move over the whole interval from sample S-8 to sample S-13.

For samples prepared at 1100 °C, the fraction of  $\alpha\text{-Fe}_2\text{O}_3$  decreased from sample S-1\* to sample S-6\* in which  $\alpha\text{-Fe}_2\text{O}_3$  was still dominant. Over the whole concentration region,  $\alpha\text{-Fe}_2\text{O}_3$  exhibited sharp diffraction lines, which did not change their angular positions with change of composition, as was also found for samples heated at a maximum temperature of 800 °C.  $\alpha\text{-Fe}_2\text{O}_3$  was not detected in sample S-7\* and in all samples up to S-12\*. Faint diffraction lines of an fcc phase, "NiFe<sub>2</sub>O<sub>4</sub>", similar to the spinel structure of NiFe<sub>2</sub>O<sub>4</sub>, appeared in sample S-2\*. This phase exhibited the unit cell parameter larger by ~ 1.0 % than that of NiFe<sub>2</sub>O<sub>4</sub>. The fraction of "NiFe<sub>2</sub>O<sub>4</sub>" increased from sample S-2\* to sample S-7\*. The important experimental fact is that diffraction lines of this phase moved towards higher Bragg angles, as the molar fraction of NiO increased from sample S-2\* to sample S-7\*. This shift corresponded to a decrease of the lattice parameter towards the value of NiFe<sub>2</sub>O<sub>4</sub>. For sample S-7\* the positions of diffraction lines corresponded to NiFe<sub>2</sub>O<sub>4</sub> and were practically equal to those obtained for sample S-7. The fraction of NiFe<sub>2</sub>O<sub>4</sub> decreased from sample S-7\* to sample S-12\*. This phase was also dominant in samples S-8\* and S-9\*. Diffraction lines of NiFe<sub>2</sub>O<sub>4</sub> did not move in the interval from samples S-7\* to S-12\*.

NiO appeared in sample S-8\* and its behaviour was similar to that in samples heated up to 800 °C. The fraction of NiO gradually increased up to sample S-13\*.

In previous papers [12, 13] we used vibrational spectroscopy to follow the chemical and structural changes in mixed metal oxides,  $\text{Fe}_2\text{O}_3$ -In<sub>2</sub>O<sub>3</sub> and  $\text{Fe}_2\text{O}_3$ -Cr<sub>2</sub>O<sub>3</sub>, which formed solid solutions. In these papers the infrared spectrum of haematite was discussed in detail.

Vibrational spectroscopy was also used in the study of spinel oxides. For instance, cobalt-substituted magnetites,  $(\text{Fe}^{3+})_A(\text{Co}_x^{2+}\text{Fe}_{1-x}^{2+}\text{Fe}^{3+})_B\text{O}_4^{2-}$ , were oxidized under controlled conditions, and the transformation of  $\gamma$ -phase to  $\alpha\text{-Fe}_2\text{O}_3$  was followed by infrared spectroscopy [15]. It was found that the defect spinels with  $x < 0.30$  showed a partial vacancy ordering at octahedral sites. On the basis of the disappearance of the infrared band at 720 cm<sup>-1</sup> of the defect  $\gamma$ -phase or the appearance of the infrared band at 470 cm<sup>-1</sup> of  $\alpha\text{-Fe}_2\text{O}_3$ , it was shown that the transition temperature  $\gamma \rightarrow \alpha$  increased with cobalt substitution. The effect of divalent cations on the formation

of  $\alpha\text{-Fe}_2\text{O}_3$  from the defect  $\gamma$ -phase was most pronounced in case of  $\text{Zn}^{2+}$ . Magnetite,  $\text{FeFe}_2\text{O}_4$ , was characterized by two infrared bands at 570 and  $370\text{ cm}^{-1}$ . For  $\text{CoFe}_2\text{O}_4$ , two characteristic infrared bands at 590 and  $383\text{ cm}^{-1}$  were found.

Ishii *et al.* [16] calculated optically active lattice vibrations of magnetite. The infrared band at  $570\text{ cm}^{-1}$  was assigned to Fe-O stretching mode,  $\nu_1(T_{1u})$ , of the tetrahedral and octahedral sites. The infrared band at  $370\text{ cm}^{-1}$  was assigned to Fe-O stretching mode,  $\nu_2(T_{1u})$ , of the octahedral sites.

In their book, Nyquist and Kagel [17] reported two characteristic infrared bands for magnetite at 570 and  $410\text{ cm}^{-1}$ .

The Raman spectra of single crystal of  $\text{NiFe}_2\text{O}_4$  and of polycrystalline  $\text{Fe}_3\text{O}_4$ ,  $\text{NiFe}_2\text{O}_4$  and  $\text{MnFe}_2\text{O}_4$ , were recorded at room temperature or at  $4.2\text{ K}$  [18]. For polycrystalline  $\text{FeFe}_2\text{O}_4$  the following Raman bands ( $\text{cm}^{-1}$ ) were observed at room temperature: 706 and 570 ( $A_{1g}$  vibrational modes), 666 and 336 ( $E_g$ ), and 490 and 226 ( $T_{2g}$ ). For polycrystalline  $\text{NiFe}_2\text{O}_4$  the following Raman bands ( $\text{cm}^{-1}$ ) were observed at room temperature: 700 and 579 ( $A_{1g}$ ), 666 and 339 ( $E_g$ ) and 490 ( $T_{2g}$ ).

Zanzucchi and Yim [19] investigated infrared emission for oxides formed on iron, nickel or Invar (36% Ni-Fe alloy). The infrared spectra of oxidized iron and 36% Ni-Fe alloy were similar. Nickel ions were not

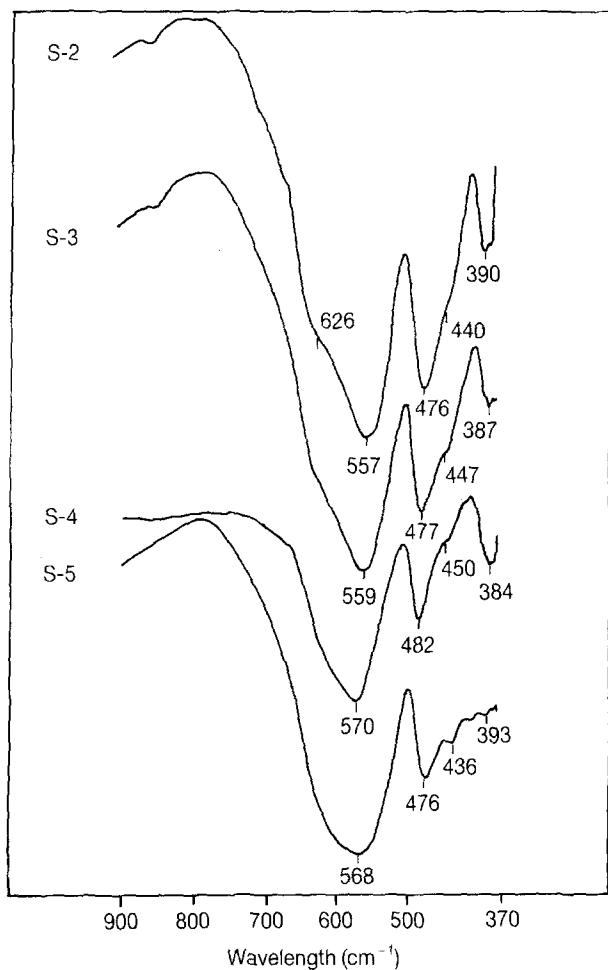


Figure 1 Fourier transform infrared spectra of samples S-2, S-3, S-4 and S-5 recorded at room temperature.

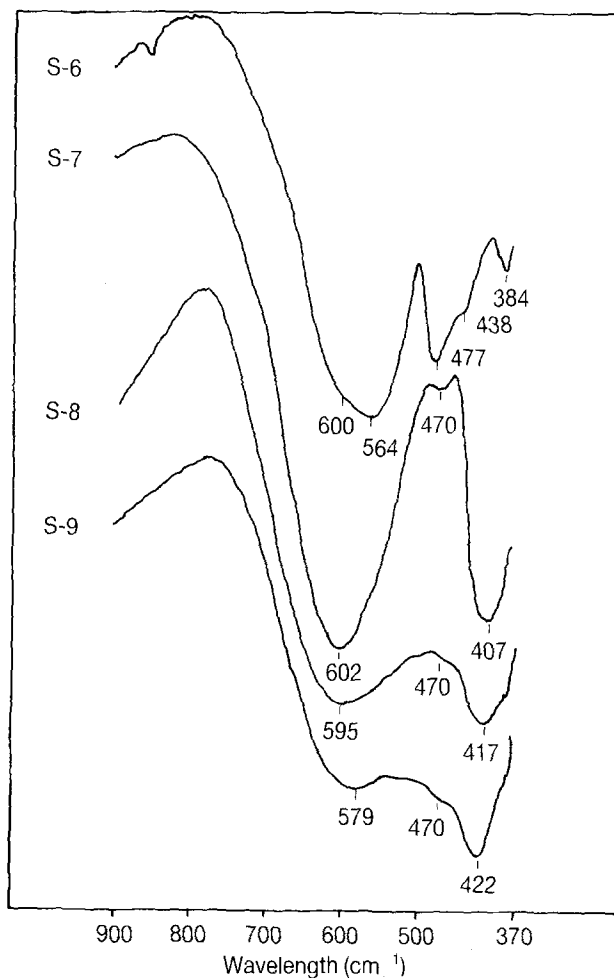


Figure 2 Fourier transform infrared spectra of samples S-6, S-7, S-8 and S-9 recorded at room temperature.

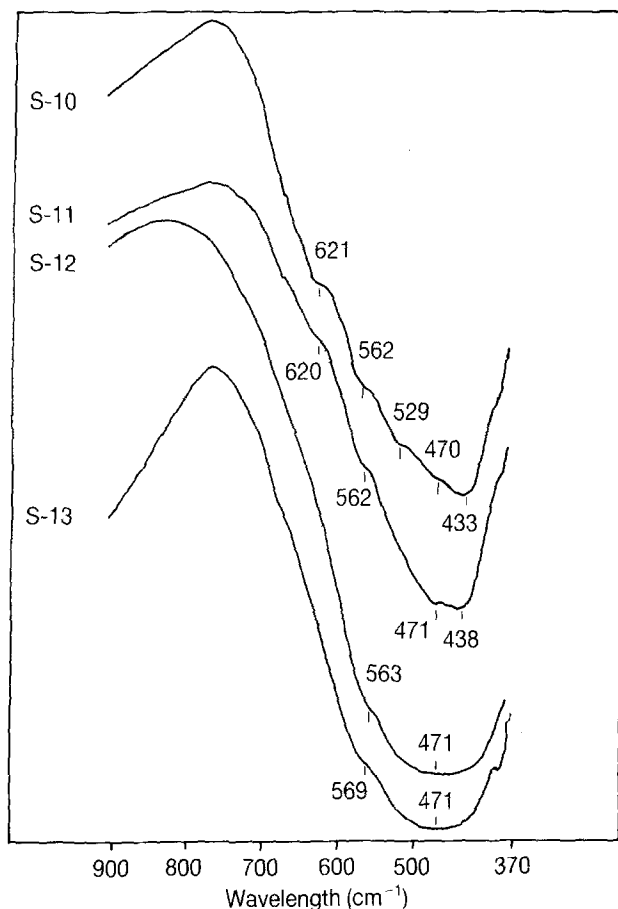


Figure 3 Fourier transform infrared spectra of samples S-10, S-11, S-12 and S-13 recorded at room temperature.

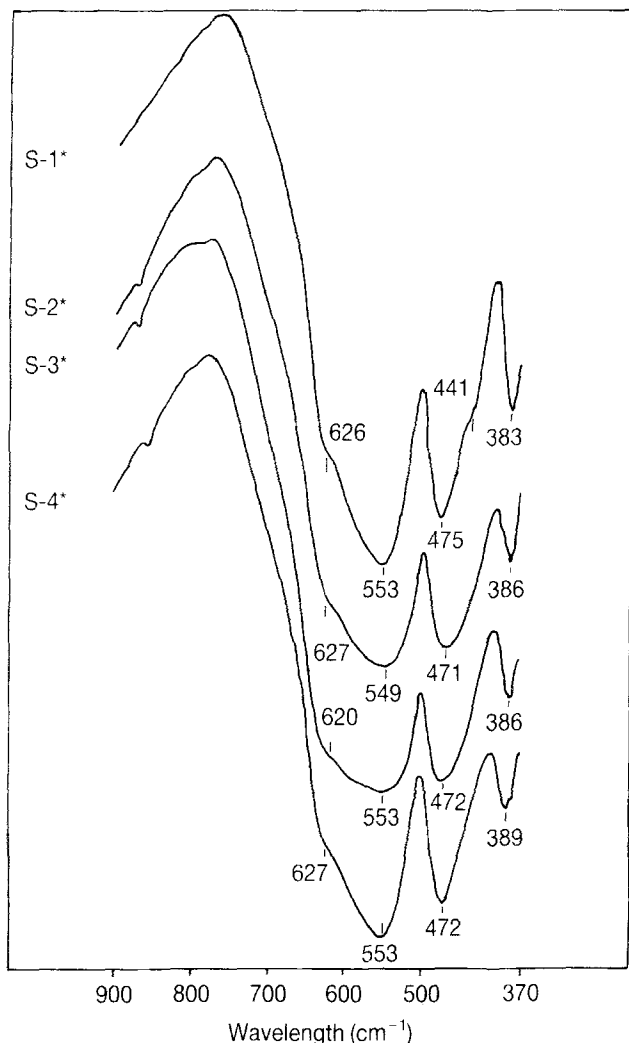


Figure 4 Fourier transform infrared spectra of samples S-1\*, S-2\*, S-3\* and S-4\* recorded at room temperature.

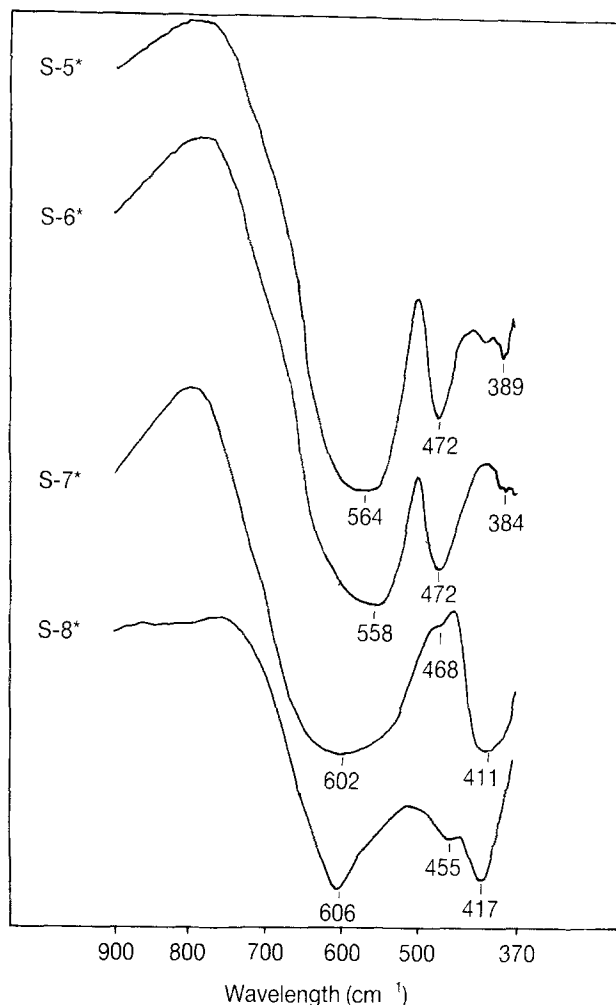


Figure 5 Fourier transform infrared spectra of samples S-5\*, S-6\*, S-7\* and S-8\* recorded at room temperature.

found in the surface layers of oxidized Invar alloy. Infrared bands of oxides of iron and nickel, from different literature sources, were summarized [19].

Infrared spectroscopy was also used to characterize nickel(II) hydroxide [20–23]. The infrared band observed in the range  $450\text{--}475\text{ cm}^{-1}$  was interpreted as the nickel–oxygen stretching vibration.

The present FT-IR spectroscopic results, obtained for samples prepared in the system  $\text{Fe}_2\text{O}_3\text{--NiO}$ , can be summarized as follows. Figs 1 and 2 show FT-IR spectra of samples S-2 to S-9. The FT-IR spectrum of sample S-2 is characterized by two dominant infrared bands at  $557$  and  $476\text{ cm}^{-1}$  and a weak intensity infrared band at  $390\text{ cm}^{-1}$ . Two shoulders at  $626$  and  $440\text{ cm}^{-1}$  are also visible. These infrared bands are typical for  $\alpha\text{-Fe}_2\text{O}_3$ . FT-IR spectra of samples S-3 and S-4 are very similar to the spectrum of sample S-2. In the FT-IR spectra of samples S-5 and S-6 the shoulders at  $436$  and  $438\text{ cm}^{-1}$  are pronounced, while the relative intensity of the infrared band at  $384\text{ cm}^{-1}$  is decreased in relation to the infrared band at  $390\text{ cm}^{-1}$ , recorded for sample S-2. The FT-IR spectrum of sample S-6 is also characterized by a broad infrared band with a transmission minimum at  $600\text{--}564\text{ cm}^{-1}$ . Two dominant infrared bands at  $602$  and  $407\text{ cm}^{-1}$  are observed in the FT-IR spectrum of

sample S-7, due to the presence of  $\text{NiFe}_2\text{O}_4$ . Changes in the FT-IR spectra of samples S-8 and S-9 can be ascribed to the appearance of NiO, characterized by an infrared band at  $470\text{ cm}^{-1}$ .

Fig. 3 shows FT-IR spectra of samples S-10 to S-13. The FT-IR spectrum of sample S-10 is characterized by a very broad infrared band with a transmission minimum at  $470\text{--}433\text{ cm}^{-1}$ . This spectrum indicates the transition from a two-phase system to a single-phase system. For the same sample, S-10, X-ray diffraction showed a broadening of diffraction lines corresponding to  $\text{NiFe}_2\text{O}_4$ . The shape of the FT-IR spectrum of sample S-11 is very similar to the previous spectrum. X-ray diffraction showed only the presence of NiO in sample S-11. On the basis of the similarity of the FT-IR spectra of samples S-10 and S-11, it can be supposed that in sample S-11, besides NiO, there is also “amorphous”  $\text{NiFe}_2\text{O}_4$ . FT-IR spectra of samples S-12 and S-13 can be ascribed to NiO. These spectra are characterized by a broad infrared band with a transmission minimum at  $471\text{ cm}^{-1}$ .

The FT-IR spectra of samples S-1\* to S-13\* are shown in Figs 4–7. The FT-IR spectrum of sample S-1\* is characterized by two dominant infrared bands at  $553$  and  $475\text{ cm}^{-1}$ , a weak intensity infrared band at  $383\text{ cm}^{-1}$  and two shoulders at  $626$  and

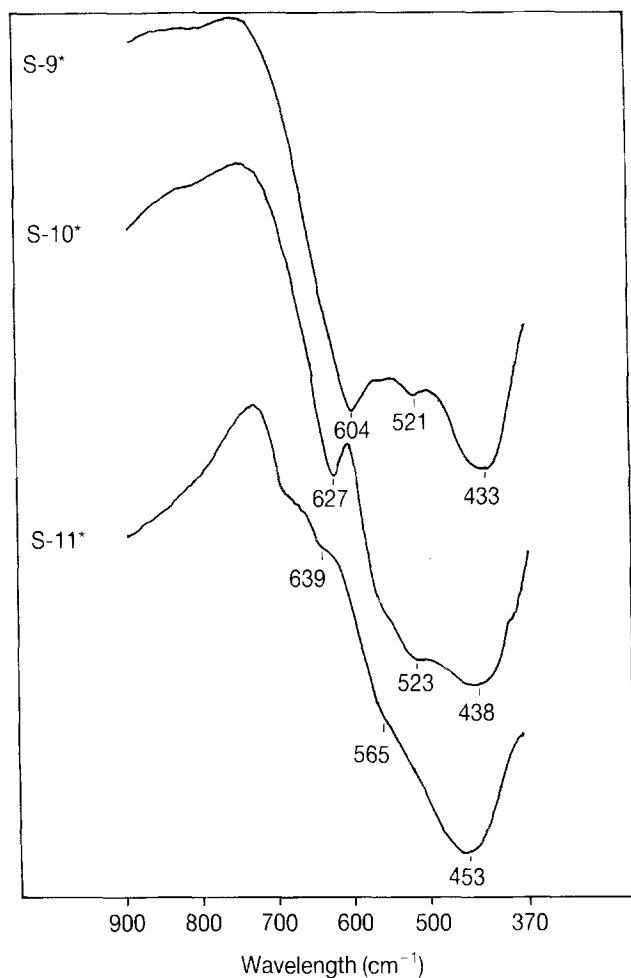


Figure 6 Fourier transform infrared spectra of samples S-9\*, S-10\* and S-11\* recorded at room temperature.

441  $\text{cm}^{-1}$ . These infrared band positions correspond to  $\alpha\text{-Fe}_2\text{O}_3$ . As the content of  $\alpha\text{-Fe}_2\text{O}_3$  decreases, there is a corresponding decrease of the relative intensity of the infrared band at 383–389  $\text{cm}^{-1}$ , and a disappearance of the shoulder at 441  $\text{cm}^{-1}$ . Sample S-7\* shows two very strong and broad infrared bands at 602 and 411  $\text{cm}^{-1}$ , due to the presence of  $\text{NiFe}_2\text{O}_4$ . A further increase of the molar fraction of NiO introduces changes in the corresponding spectra. In the FT-IR spectrum of sample S-8\*, the infrared bands corresponding to  $\text{NiFe}_2\text{O}_4$ , are shifted to 606 and 417  $\text{cm}^{-1}$ . The infrared band appearing originally at 602  $\text{cm}^{-1}$  for sample S-7\* becomes a shoulder at 639  $\text{cm}^{-1}$  for sample S-11\*, while the infrared band originally at 411  $\text{cm}^{-1}$  for sample S-7\* overlaps the infrared band which corresponds to NiO. FT-IR spectrum of pure NiO prepared at 1100 °C (sample S-13\*) is characterized by a broad infrared band with a transmission minimum at 466  $\text{cm}^{-1}$ .

## References

1. V. SITAKARA RAO, S. RAJENDRAN and H. S. MAITI, *J. Mater. Sci.* **19** (1984) 3593.
2. Y. TAMAURA, T. SASAO, M. ABE and T. ITOH, *J. Colloid Interface Sci.* **136** (1990) 242.
3. A. M. GADALLA and H.-F. YU, *J. Mater. Res.* **5** (1990) 2923.
4. A. A. IBRAHIM and G. A. EL-SHOBAKY, *Thermochim. Acta* **132** (1988) 117.
5. K. J. D. MacKENZIE and C. M. CARDILE, *ibid.* **165** (1990) 207.

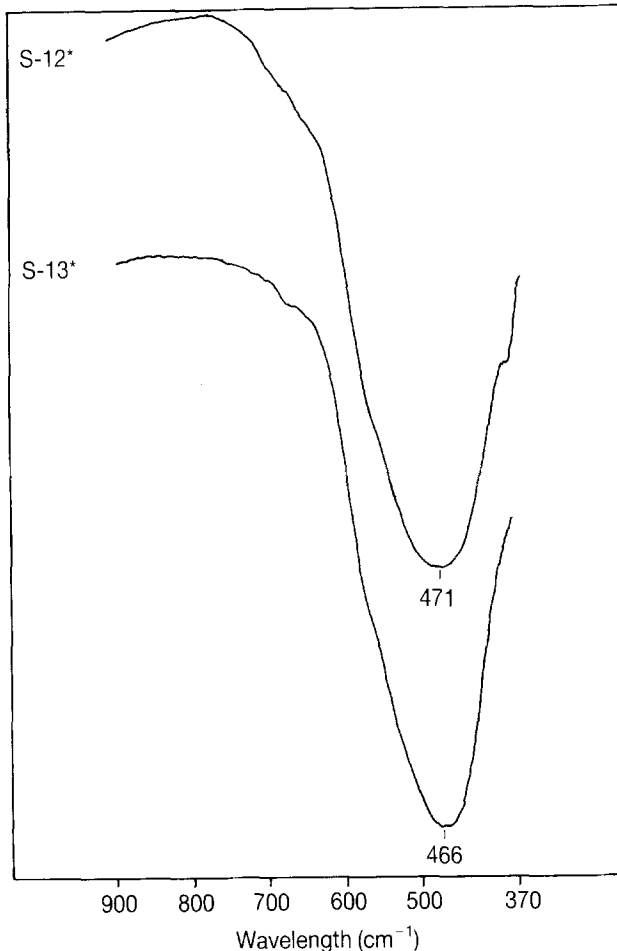


Figure 7 Fourier transform infrared spectra of samples S-12\* and S-13\* recorded at room temperature.

6. H. S. MAITI, S. RAJENDRAN and V. SITAKARA RAO, *Phys. Status Solidi (a)* **84** (1984) 631.
7. A. H. MORRISH and K. HANEDA, *J. Appl. Phys.* **52** (1981) 2496.
8. K. HANEDA, H. KOJIMA and A. H. MORRISH, *J. Magn. Mater.* **31–34** (1983) 951.
9. A. H. MORRISH and K. HANEDA, *ibid.* **35** (1983) 105.
10. G. C. ALLEN, J. A. JUTSON and P. A. TEMPEST, *J. Nucl. Mater.* **158** (1988) 96.
11. M. LENGLET, R. GUILLAMET, J. LOPITAUX and B. HANNOYER, *Mater. Res. Bull.* **25** (1990) 575.
12. M. RISTIĆ, S. POPOVIĆ, M. TONKOVIĆ and S. MUSIĆ, *J. Mater. Sci.* **26** (1991) 4225.
13. S. MUSIĆ, S. POPOVIĆ and M. RISTIĆ, *ibid.*, in press.
14. International Centre for Diffraction Data, Joint Committee on Powder Diffraction Standards, Powder diffraction file, 1601 Park Lane, Swarthmore, PA 19081, USA.
15. B. GILLOT, F. JEMMALI and A. ROUSSET, *J. Solid State Chem.* **50** (1983) 138.
16. M. ISHII, M. NAKAHIRA and T. YAMANAKA, *Solid State Commun.* **11** (1972) 209.
17. R. A. NYQUIST and R. O. KAGEL, "Infrared Spectra of Inorganic Compounds" (Academic Press, New York, London, 1971).
18. P. R. GRAVES, C. JOHNSTON and J. J. CAMPANIELLO, *Mater. Res. Bull.* **23** (1988) 1651.
19. P. J. ZANZUCCHI and M. W. YIM, *Appl. Spectr.* **40** (1986) 1042.
20. F. P. KOBER, *J. Electrochem. Soc.* **112** (1965) 1064.
21. *Idem.*, *ibid.* **114** (1967) 215.
22. N. MINKOVA, M. KRUSTEVA and G. NIKOLOV, *J. Molec. Struct.* **115** (1984) 23.
23. T. S. HORÁNYI, *Thermochim. Acta* **142** (1989) 143.

Received 30 September 1991  
and accepted 16 June 1992